Atomic layer deposition by reaction of molecular oxygen with tetrakisdimethylamido-metal precursors

J Provine, Peter Schindler, Jan Torgersen, and Hyo Jin KimHans-Peter KarnthalerFritz B. Prinz

Citation: Journal of Vacuum Science & Technology A: Vacuum, Surfaces, and Films **34**, 01A138 (2016); doi: 10.1116/1.4937991

View online: http://dx.doi.org/10.1116/1.4937991

View Table of Contents: http://avs.scitation.org/toc/jva/34/1

Published by the American Vacuum Society

Articles you may be interested in

Review Article: Recommended reading list of early publications on atomic layer deposition—Outcome of the "Virtual Project on the History of ALD"
Journal of Vacuum Science & Technology A: Vacuum, Surfaces, and Films **35**, 010801010801 (2016); 10.1116/1.4971389

Overview of atomic layer etching in the semiconductor industry
Journal of Vacuum Science & Technology A: Vacuum, Surfaces, and Films **33**, 020802020802 (2015); 10.1116/1.4913379

Correlation of film density and wet etch rate in hydrofluoric acid of plasma enhanced atomic layer deposited silicon nitride
Journal of Vacuum Science & Technology A: Vacuum, Surfaces, and Films **6**, 065012065012 (2016); 10.1063/1.4954238

Quasi-atomic layer etching of silicon nitride
Journal of Vacuum Science & Technology A: Vacuum, Surfaces, and Films **35**, 01A10201A102 (2016); 10.1116/1.4967236

Instruments for Advanced Science

Contact Hiden Analytical for further details:
W www.HidenAnalytical.com
E info@hiden.co.uk
CLICK TO VIEW our product catalogue

Gas Analysis
- dynamic measurement of reaction gas streams
- catalysis and thermal analysis
- molecular beam studies
- dissolved species probes
- fermentation, environmental and ecological studies

Surface Science
- UHV TPD
- SIMS
- end point detection in ion beam etch
- elemental imaging - surface mapping

Plasma Diagnostics
- plasma source characterization
etch and deposition process reaction
- kinetic studies
- analysis of neutral and radical species

Vacuum Analysis
- partial pressure measurement and control of process gases
- reactive sputter process control
- vacuum diagnostics
- vacuum coating process monitoring

CrossMark
click for updates

Atomic layer deposition by reaction of molecular oxygen with tetrakisdimethylamido-metal precursors

J Provine,[a),b)] Peter Schindler,[a)] Jan Torgersen, and Hyo Jin Kim
Department of Mechanical Engineering, Stanford University, Stanford, California 94305

Hans-Peter Karnthaler
Physics of Nanostructured Materials, University of Vienna, 1090 Vienna, Austria

Fritz B. Prinz
Department of Mechanical Engineering, Stanford University, Stanford, California 94305 and Department of Materials Science and Engineering, Stanford University, Stanford, California 94305

(Received 6 September 2015; accepted 1 December 2015; published 21 December 2015)

Tetrakisdimethylamido (TDMA) based precursors are commonly used to deposit metal oxides such as TiO_2, ZrO_2, and HfO_2 by means of chemical vapor deposition and atomic layer deposition (ALD). Both thermal and plasma enhanced ALD (PEALD) have been demonstrated with TDMA-metal precursors. While the reactions of TDMA-type precursors with water and oxygen plasma have been studied in the past, their reactivity with pure O_2 has been overlooked. This paper reports on experimental evaluation of the reaction of molecular oxygen (O_2) and several metal organic precursors based on TDMA ligands. The effect of O_2 exposure duration and substrate temperature on deposition and film morphology is evaluated and compared to thermal reactions with H_2O and PEALD with O_2 plasma. © *2015 American Vacuum Society*. [http://dx.doi.org/10.1116/1.4937991]

I. INTRODUCTION

Thin films of TiO_2, HfO_2, and ZrO_2 are commonly used in many application such as high-*k* gate dielectrics,[1] resistive memory,[2] and corrosion barriers.[3] Atomic layer deposition (ALD) is the key enabling technique to deposit thin films conformally and pinhole-free with thickness control down to the Angstrom scale. Tetrakisdimethylamido (TDMA) complexes have been added to several metals to create precursors for CVD and ALD. This includes, but is not limited to, TDMA-Ti,[4,5] TDMA-Hf,[6] TDMA-Zr,[6] and TDMA-Sn.[7] Each of these precursors has been extensively used for ALD of metal oxides, typically through interaction with water vapor for a thermal process or in a plasma enhanced process utilizing an O_2 plasma.

While ALD and plasma-enhanced ALD (PEALD) of these TDMA-based precursors to form binary oxides have been extensively studied in the past, their reactivity with pure oxygen alone has been only scarcely discussed in literature till date. The thermal decomposition of TDMA-Hf and its effect on film growth with molecular O_2 at different temperatures has been explored previously.[8] However, a detailed study on the effect of O_2 dose has not been conducted. The TDMA-ligands being reactive to molecular oxygen may enable ALD of these metal oxides for processes where H_2O would not be desirable or where the conformality limitations of PEALD are detrimental. Furthermore, recognizing this feature of TDMA-type precursors is crucial to prevent undesired deposition in a system without sufficient protection against stray oxygen contamination.

In this paper, we utilize a Cambridge Nanotech/Ultratech Fiji F200 system using TDMA-Ti, TDMA-Hf, and TDMA-Zr as precursors to deposit TiO_2, HfO_2, and ZrO_2, respectively. As anticipated, each precursor was successfully able to deposit their respective oxide through a plasma O_2 process or a thermal process when reacted with H_2O vapor. However, each precursor was also found to react with molecular oxygen. This report explores the reaction of TDMA-based precursors with oxygen and the effect of O_2 dose and temperature on the growth behavior in detail. High resolution TEM (HRTEM) and grazing incidence x-ray diffraction (GIXRD) data reveal structural information of the deposited layers. X-ray photoelectron spectroscopy (XPS) shows that the deposited films that utilize only pure oxygen as a coreactant are free of carbon and nitrogen contamination and yield stoichiometric films. We further show that depending on the presence of plasma and the O_2 duration during the second half-cycle, the film's morphology and density can be tuned.

II. EXPERIMENTAL PROCEDURE

A. Material fabrication

Utilizing a Cambridge Nanotech/Ultratech Fiji F200 system that is equipped with a remote inductively coupled plasma (ICP) generator, we evaluated TDMA-Ti, TDMA-Hf, and TDMA-Zr to deposit TiO_2, HfO_2, and ZrO_2, respectively. The TDMA-type precursors were maintained at 75 °C and were pulsed for 0.25 s (TDMA-Hf) and 0.3 s (TDMA-Ti and TDMA-Zr). Pure oxygen (30 sccm flow) with and without the ICP turned on (plasma power 300 W) was used for the oxidation half-cycle. The base pressure of this ALD reactor is 200 mTorr while there is a constant flow of Ar at 30 sccm in the precursor manifold line and 110 sccm in the plasma line. The chamber was purged with Ar for 20 s after the precursor half-cycle and for 5 s after the oxidation half-cycle. Additionally, thermal ALD films were grown using H_2O vapor as an oxidant with a pulse time of 0.06 s. Boron

[a)]J. Provine and P. Schindler contributed equally to this work.
[b)]Electronic mail: jprovine@stanford.edu

 © 2015 American Vacuum Society

doped (100) Si wafers were used as substrates and were RCA-cleaned immediately prior to each deposition.

Since each of the precursors under consideration are known to react with water vapor, significant care was undertaken to ensure that the reactions under observation were not affected by stray moisture in the system. There are three sources of potential moisture contamination to consider in evaluating the system: (1) general leaks or residual moisture in the deposition chamber, (2) the Ar carrier gas used in the system for fluidic transfer of precursors and purging, and (3) the O_2 process gas used as the oxidant. Electronic grade ultrahigh purity Ar and O_2 sources were used for all experiments. As a first test, trimethylaluminum (TMA) was pulsed into the reaction chamber with a Si substrate present while not introducing an oxidant. TMA is highly reactive with H_2O and nonreactive with molecular O_2 at the temperature range in consideration (tests performed at 200 °C). A growth per cycle (GPC) of <0.02 Å/cycle was measured for 100 cycles of TMA pulses, indicating that the system and Ar carrier gas contained no moisture. Next, the above experiment was repeated with O_2 flowing at 30 sccm for 60 s for each ALD cycle. Again, a GPC of <0.02 Å/cycle was measured, indicating a lack of moisture in the O_2 process gas line. Finally, for a thorough double check, we ran 500 cycles of TDMA-Ti precursor pulses with a 60 s purge time per cycle without flowing any O_2. The GPC was measured as <0.01 Å/cycle, which confirms again the lack of moisture in the system and Ar carrier gas.

B. Material characterization

The film thickness was measured using spectroscopic ellipsometry (Woollam M2000). Additionally, x-ray reflectivity (XRR) measurements were carried out (X'Pert Pro, PANalytical) to confirm the film thickness and obtain further insight into the density of the film. GIXRD was employed to analyze the crystalline modification of the thin films. Grazing angle was set to 1°. HRTEM at an acceleration voltage of 300 kV was employed to confirm the structure and morphology of the films (FEI Titan ETEM 300 kV). Cross-sectional TEM samples were prepared by a conventional polishing approach, and in the final step, gentle ion polishing is applied using a Gatan PIPS2. The composition analysis was conducted using XPS (PHI VersaProbe Scanning XPS Microscope).

III. RESULTS AND DISCUSSION

The GPC of TDMA-Hf, TDMA-Ti, and TDMA-Zr using different oxidants is plotted as a function of oxidant duration in Figs. 1(a)–1(c), respectively. For comparison, both pure oxygen and oxygen plasma were used with the duration of 15 and 60 s. The GPC of the thermal ALD process using water vapor is also indicated in Fig. 1. All samples displayed in Fig. 1 were deposited at 200 °C. The GPC of the various experiments is summarized in Table I.

The reactivity with molecular O_2 is much reduced in comparison with O_2 plasma or H_2O, which is evident through the GPC exhibited being significantly lower than the

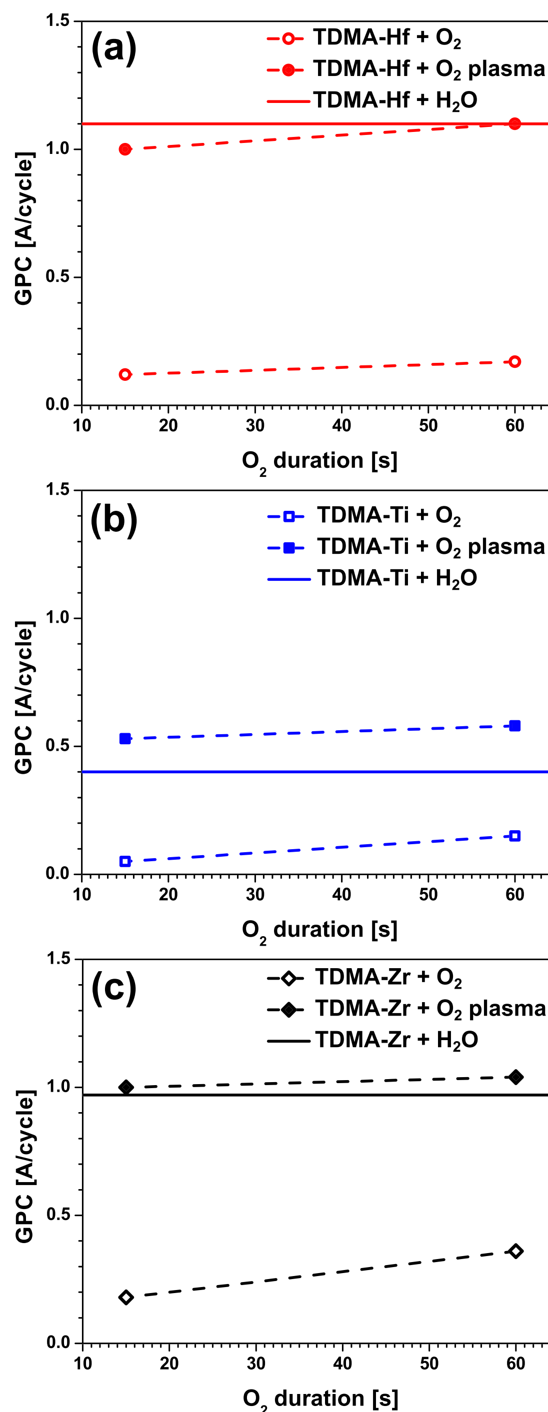

Fig. 1. (Color online) GPC as a function of O_2 duration during the oxidation half-cycle is plotted for HfO_2, TiO_2, and ZrO_2 in (a)–(c), respectively. Open symbols correspond to the ICP being turned off, whereas closed symbols signify the ICP being turned on. The solid line indicates the GPC of the thermal ALD case where water is used as an oxidant. Substrate temperature was set at 200 °C for all samples. In each deposition, sufficient cycles were run to deposit a film with thickness on the order of 100 Å, with GPC values and thicknesses listed in Table I.

saturated GPC. Extended O_2 duration in both cases increased the GPC slightly. The values reported for PEALD and thermal ALD of the deposited binary metal oxides are consistent with previous experiments carried out at the Stanford Nanofabrication Facility and reports in literature.[8,9] It is

TABLE I. GPC and film thickness measurements for TDMA-Hf/Ti/Zr by PEALD, thermal ALD with molecular O_2, and thermal ALD with water vapor. The thickness for each sample is provided in parentheses after the GPC. Substrate temperature was set at 200 °C for all samples.

	Molecular O_2		Plasma O_2		
Precursor	15 s	60 s	15 s	60 s	Thermal ALD
TDMA-Hf	0.12 ± 0.004 Å (57.5 Å)	0.17 ± 0.005 Å (66.0 Å)	1.00 ± 0.02 Å (100.3 Å)	1.10 ± 0.01 Å (221 Å)	1.10 ± 0.02 Å (112 Å)
TDMA-Ti	0.05 ± 0.004 Å (27.0 Å)	0.15 ± 0.004 Å (71.5 Å)	0.53 ± 0.01 Å (105 Å)	0.57 ± 0.01 Å (113 Å)	0.40 ± 0.008 Å (99.7 Å)
TDMA-Zr	0.18 ± 0.004 Å (88.3 Å)	0.36 ± 0.004 Å (182 Å)	1.00 ± 0.01 Å (201 Å)	1.04 ± 0.01 Å (208 Å)	0.97 ± 0.02 Å (96.7 Å)

again important to note that great care was undertaken to ensure that the reactions under observation were not affected by stray moisture in the system (as discussed in detail in Sec. II). This information has not been provided in previous work by Kim *et al*. that reports a GPC close to the thermal ALD saturation rate (of ∼1 Å/cycle) for TDMA-Hf with 6 s of O_2 exposure per cycle at 200 °C (while we have measured a GPC of <0.2 Å/cycle after 60 s of O_2 exposure per cycle).[8]

XPS and XRR measurements were carried out to analyze the composition and density of the films. All films in this study deposited by reaction of TDMA-based precursors and molecular oxygen showed negligible contamination by nitrogen or carbon. Further all films were found to have stoichiometry equivalent to X:O 1:2, with X as the relevant metal attached to the TDMA precursor structure. An example of the XPS data is provided in the supplementary material.[10] Utilizing XRR, the density of the various metal oxide films was measured, and the results are summarized in Table II. The films reacted with molecular O_2 show reduced density compared to either PEALD or water based thermal ALD. Further, extension of the O_2 dosage increases the density of both TiO_2 and HfO_2 films while ZrO_2 film density remains constant.

To gain further insight into the deposition of TDMA-based precursors using molecular oxygen, we performed depositions with detailed conditions for the case of TDMA-Ti. The GPC as a function of O_2 duration (at a fixed substrate temperature of 200 °C) and as a function of substrate temperature (at a fixed oxidant duration per cycle of 60 s) are plotted in Figs. 2(a) and 2(b), respectively. The thickness of the deposited film with increasing numbers of cycles is displayed in Fig. 2(c).

The results in Fig. 2(a) show that the GPC is still not saturated even at a long O_2 exposure time of 180 s per cycle but begins to level off. Considering the deposition is not fully

TABLE II. Density values (in g/cm^3) for TDMA-Hf/Ti/Zr by PEALD, thermal ALD with molecular O_2, and thermal ALD with water. Substrate temperature was set at 200 °C for all samples.

	Molecular O_2		Plasma O_2		
Precursor	15 s	60 s	15 s	60 s	Thermal ALD
TDMA-Hf	5.2	6.7	7.8	7.7	7.5
TDMA-Ti	3.0	3.7	3.5	3.7	3.9
TDMA-Zr	4.5	4.5	5.6	5.4	5.7

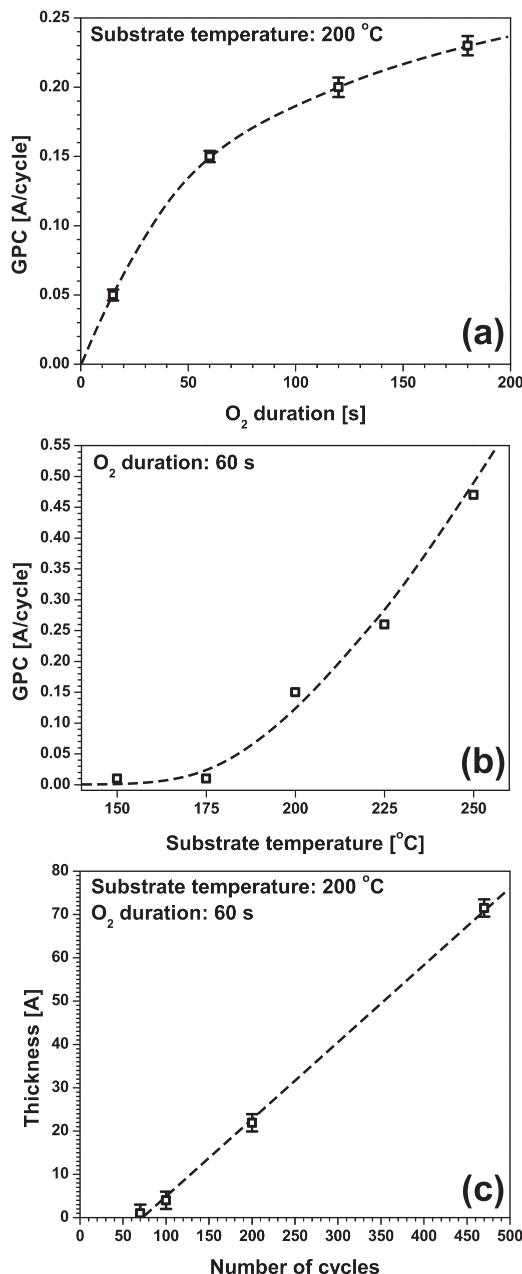

FIG. 2. TDMA-Ti growth characteristics with pure O_2 are plotted. (a) GPC as a function of O_2 duration at 200 °C substrate temperature. (b) GPC as a function of substrate temperature for a fixed O_2 duration of 60 s per cycle. (c) Thickness of TiO_2 measured for different numbers of cycles at a substrate temperature of 200 °C and an O_2 duration of 60 s per cycle.

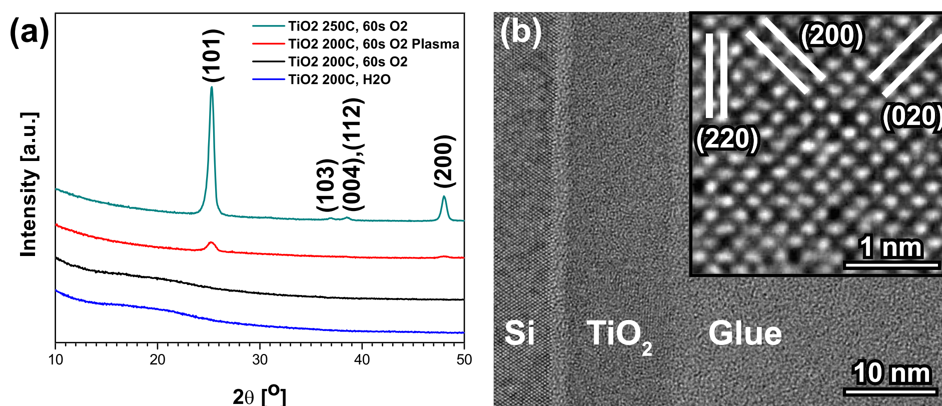

Fig. 3. (Color online) (a) GIXRD patterns of TiO_2 deposited at different temperatures and oxidant conditions: 200 °C using water, 60 s O_2 and 60 s O_2 plasma, as well as at 250 °C using molecular O_2. Anatase peaks are labeled. (b) Cross-sectional TEM of TiO_2 deposited on a Si wafer at 200 °C and 60 s O_2 is displayed. The inset shows an aberration-corrected HRTEM micrograph indicating the (200), (020), and (220) planes of Anatase.

saturated, it is technically inappropriate to refer to the depositions as ALD. The leveling off of the GPC with increased O_2 exposure indicates that saturation may happen eventually, though only for lengthy cycle times. We continue with the convention of describing the deposition as ALD because of the self-limiting surface saturation of TDMA-type precursors, but note that the oxidant half-reaction is not complete at the exposure dosages explored. The excellent step coverage on high aspect-ratio substrates is a further indicator that the reaction involved is self-limiting (as observed in Fig. 4). Figure 2(b) indicates that the process is thermally activated showing an exponential increase in GPC with increasing temperature, following a traditional Arrhenius relationship. The activation energy associated with the ALD cycle reactions are calculated from Fig. 2(b) and included in the supplementary material. The thickness of the grown film increases linearly after an initial nucleation phase that takes about 60 cycles.

To study the effect of oxidant type and temperature on the structure of the film, we used GIXRD and cross-sectional TEM of TiO_2 deposited at various deposition conditions. Figure 3(a) plots GIXRD patterns of TiO_2 deposited at 200 °C using H_2O, 60 s molecular O_2, and 60 s O_2 plasma as an oxidant and at 250 °C using 60 s molecular O_2. The thickness of each of these films is as follows: deposition at 200 °C using H_2O (99.7 Å), 60 s molecular O_2 (71.5 Å), and 60 s O_2 plasma (113 Å) as an oxidant and at 250 °C using 60 s molecular O_2 (235 Å). At 200 °C deposition temperature, the film is amorphous when water or molecular oxygen is used as an oxidant but has a crystalline phase (peaks from the Anatase phase start to emerge) in the case of O_2 plasma. Interestingly, at 250 °C deposition temperature and 60 s molecular O_2 as oxidant, the GIXRD pattern shows strong crystalline peaks corresponding to the Anatase phase. The observed Anatase peaks are (101), (103), (004) and (112), and (200) at 25.3°, 36.9°, 37.8° and 38.6°, and 48.0°, respectively. To confirm the film's crystallinity at 250 °C deposition temperature and 60 s O_2 for the oxidation half-cycle, the cross-sectional TEM was carried out, as shown in Fig. 3(b). The inset displays an aberration-corrected HRTEM micrograph confirming the Anatase phase of TiO_2. The crystalline planes were measured as 2.0 and 1.4 A in agreement with the (200)/(020) and (220) planes of the Anatase phase.

In agreement with previous literature, Anatase is the dominant phase for TiO_2 deposited by ALD with a TDMA-type precursor.[11] The observation that TiO_2 is amorphous when pure O_2 is used and mainly crystalline when O_2 plasma is used (at the same temperature) might be explained by the excited nature of the plasma species that give rise to additional energy available for crystallization. As expected, the substrate temperature plays a role in crystallinity in the thin film, though both time of oxidation and plasma input can contribute to crystallite formation in the film. Further GIXRD measurements for TiO_2, ZrO_2, and HfO_2 films may be found in the supplementary material.

Using molecular oxygen as an oxidant for ALD might be interesting for the application of depositing conformally on high aspect-ratio (AR) substrates due to no recombination losses of unexcited species of O_2 down such structures. Previously, an extension of the in-cycle plasma time was shown to improve the step coverage of PEALD TiO_2 films using a TDMA-Ti precursor.[11] The step coverage is defined as the thickness measured at the bottom of a high AR surface divided by the thickness measured at the top, in percentage.

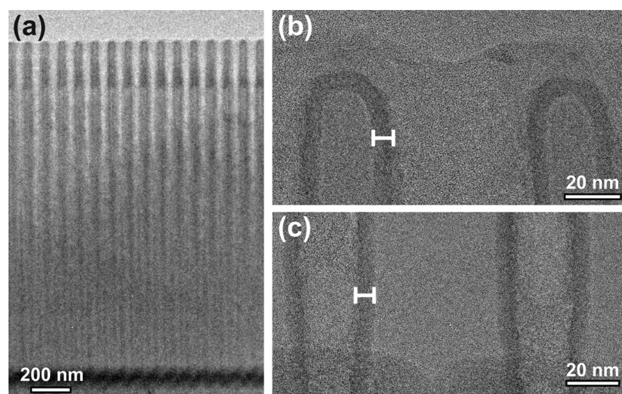

Fig. 4. (a) Low magnification cross-sectional TEM micrograph showing TiO_2 deposited on a high AR trench substrate. (b) and (c) TiO_2 at top and bottom of the trenchlike substrate in higher magnification, respectively. The location where the thickness was measured is indicated by a white bar.

TABLE III. Bond dissociation energies of tetrakisdimethylamido ligands to the metal centers Ti, Zr, and Hf, respectively. *Ab initio* calculations using Gaussian09 (details of the simulation can be found in the supplementary material).

Bond dissociation energies (eV)	TDMA-Ti	TDMA-Zr	TDMA-Hf
First ligand	3.11	3.35	3.69
Second ligand	3.26	3.67	4.13
Third ligand	3.81	3.78	4.36
Fourth ligand	4.4	4.38	3.65

Hence, a sample was fabricated using 300 cycles of TDMA-Ti precursor and an O_2 duration (without plasma) of 180 s at a substrate temperature of 200 °C. The substrate that is used in this work consists of trenches (i.e., cylindrical holes) that have a diameter of about 55 nm and a depth of 1600 nm, giving a high AR of 1:30. The morphology of the trenches resembles a conical cylinder that reduces in diameter with depth. Cross-sectional TEM of this substrate with TiO_2 is displayed in Fig. 4(a). The thickness measured (average over five different positions) at the top [as indicated in Fig. 4(b)] and bottom [Fig. 4(c)] was measured to be 6.73 ± 0.17 and 6.57 ± 0.16 nm, respectively. This yields a step-coverage of 97.7 ± 2.4%.

In an effort to understand the mechanism behind the chemical reactions observed through the experiments presented above, *ab initio* simulations were utilized. A full simulation of the myriad reaction pathways possible in this system is beyond the scope of this work; so, we instead limited our analysis to calculations of the bond dissociation energies. According to Ref. 12, precursors with high dissociation energies require sufficient vapor and thermal energy to adsorb on the surface and generally have a low GPC. Precursors with low bond dissociation energies may enhance the GPC at higher growth temperatures due to the CVD-like growth of films. The theoretical bond dissociation energies of the TDMA-X precursors are comparably high for ALD precursors (see Table III).[13]

At similar precursor doses, precursor and substrate temperatures, a reaction with H_2O and or O_2 plasma results in a ALD growth behavior with no observable thermal decomposition. Without O_2, we do not observe any deposition (see Sec. II). An excellent step coverage was obtained on a 1:30 aspect ratio trench substrate (Fig. 4). These findings suggest that the TDMA-X precursor in this work did not thermally decompose but rather likely reacted with molecular O_2.

IV. CONCLUSION

In summary, we have shown that multiple TDMA-based organometallic precursors have measurable reactivities with molecular oxygen, creating the possibility of thermal atomic layer deposition with a water free process. Further, we evaluated these films concerning the effect of oxygen dose and substrate temperature. The deposited films were found to be of high purity and free of contaminants from unreacted ligands and of tunable morphology and density. Further, we showed an almost perfect step coverage for TiO_2 deposited on a 1:30 high AR substrate. This result may be of use for ALD metal oxide processes in which the use of H_2O is undesirable but which require extremely conformal deposition. Regardless, it is a key bit of knowledge to understand to prevent undesired CVD in a system without sufficient protection against stray oxygen contamination.

ACKNOWLEDGMENTS

This work was performed at the Stanford Nano Shared Facilities and Stanford Nanofabrication Facility at Stanford University. Furthermore, J.T. acknowledges the financial support of the Austrian Science Fund (FWF) under the Contract No. J3505-N20.

[1]E. P. Gusev, C. Cabral, M. Copel, C. D'Emic, and M. Gribelyuk, Microelectron. Eng. **69**, 145 (2003).
[2]B. Chakrabarti, R. V. Galatage, and E. M. Vogel, IEEE Electron Device Lett. **34**, 867 (2013).
[3]A. J. Haemmerli, J. C. Doll, J. Provine, R. T. Howe, D. Golhaber-Gordon, and B. L. Pruitt, *17th International Conference on Solid-State Sensors, Actuators, and Microsystems*, Barcelona, Spain, 16-20 June (2013).
[4]D.-H. Kim, J. J. Kim, J. W. Park, and J. J. Kim, J. Electrochem. Soc. **143**, 9 (1996).
[5]Q. Xie, Y.-L. Jiang, C. Detavernier, D. Deduytsche, R. L. Van Meirhaeghe, G.-P. Ru, B.-Z. Li, and X.-P. Qu, J. Appl. Phys. **102**, 083521 (2007).
[6]D. M. Hausmann, E. Kim, J. Becker, and R. G. Gordon, Chem. Mater. **14**, 4350 (2002).
[7]J. W. Elam, D. A. Baker, A. J. Hryn, A. B. F. Martinson, M. J. Pellin, and J. T. Hupp, J. Am. Vac. Soc., A **26**, 244 (2008).
[8]J. C. Kim, Y. S. Cho, and S. H. Moon, Jpn. J. Appl. Phys. **48**, 066515 (2009).
[9]J. W. Lim, S. J. Yun, and J. H. Lee, Electrochem. Solid-State Lett. **7**, F73 (2004).
[10]See supplementary material in http://dx.doi.org/10.1116/1.4937991 for GIXRD results, activation energy calculation, and ab-initio simulation details.
[11]P. Schindler, M. Logar, J. Provine, and F. B. Prinz, ACS Langmuir **31**, 5057 (2015).
[12]S. W. Lee *et al.*, Chem. Mater. **23**, 2227 (2011).
[13]T. P. Holme and F. B. Prinz, J. Phys. Chem. A **111**, 8147 (2007).